Supplemental Figure Legends

Figure S1: Enteric glial elimination in Plp1^{CreER};Rosa26^{DTA} mice is dependent on the presence of both Cre recombinase and tamoxifen.

(A-D) Neurofilament-H (NF-H) and S100β immunoreactivities in the colons of Rosa26^{DTA} (Cre^{-}, control) and Plp1^{CreER};Rosa26^{DTA} mice (Cre^{+}, experimental), imaged at focal plane of the myenteric plexus. Glial loss is Cre-dependent.

(E-F) NF-H and S100β immunoreactivities in the colon of Plp1^{CreER};Rosa26^{DTA} mice (Cre^{+}) imaged at focal plane of the myenteric plexus. There is no glial loss in Cre^{+} mice in the absence of tamoxifen treatment. Scale bar = 50μm

Figure S2: Enteric glial elimination in Plp1^{CreER};Rosa26^{DTA} mice does not cause histological evidence of intestinal inflammation.

Hematoxylin and eosin stained cross-sections of duodenums, ilea and colons from Cre^{-} (control) and Cre^{+} (glial-ablated) mice at 7, 11 and 14 days post-tamoxifen treatment (dpt) reveal no evidence of inflammation. Representative images from at least 4-5 mice examined per condition.

Figure S3: Valganciclovir treatment of GFAP$^{HSV\text{-}TK}$ mice leads to extensive injury to non-targeted cells; this non-specific toxicity is not observed in Plp1^{CreER};Rosa26^{DTA} mice.

(A-B) HSV-TK and phosphorylated histone 2AX (pH2AX) immunoreactivities imaged at the level of the myenteric plexus in ilea from TK^{-} (A) and TK^{+} (B) mice treated with valganciclovir (VGCV). Neither HSV-TK, nor pH2AX immunoreactivities are evident in control tissue (A); however, abundant transgene expression (magenta) and apoptosis (green) can be seen in the experimental TK^{+} mouse tissue (B). Although many of the apoptotic cells display simultaneous transgene expression, some apoptotic cells express only pH2AX (arrows) suggesting that toxicity is not limited to transgene-expressing cells. Nuclei counterstained with TO-PRO3 (blue). Scale bar = 50μm

(C-D) The ultrastructure of bundles of nerve fibers in interganglionic connectives from the small intestines of VGCV-treated TK^{-} (C) and TK^{+} (D) mice. Note that the glial sheath completely envelops the connective in the control preparation (C), partitions groups of axons, and maintains a tightly packed order among the axons. Following glial ablation (D) the perineuronal glial sheath is deficient, gaps appear within the connective, the order of the connective is disrupted, and many axons are in direct contact with the

surrounding connective tissue. Some of the neurites (arrows) appear to be vacuolated and the cytoplasm of some axons is increased in electron density (*). Scale bars = 500 nm

(E-F) Phosphorylated histone 2AX (pH2AX) immunoreactivity does not differ in the ilea of $Rosa26^{DTA}$ (Cre^{-}, control) and $Plp1^{CreER}$;$Rosa26^{DTA}$ mice (Cre^{+}, experimental). Nuclei are counterstained with DAPI. Scale bar = 50µm

Supplemental Table 1: Mouse Lines

Mouse Line	JAX Stock	Reference
$Plp1^{CreER}$	005975	Doerflinger NH, Macklin WB, Popko B. Inducible site-specific recombination in myelinating cells. Genesis 2003;35:63-72.
$Rosa26^{DTA}$	009669	Voehringer D, Liang HE, Locksley RM. Homeostasis and effector function of lymphopenia-induced "memory-like" T cells in constitutively T cell-depleted mice. J Immunology 2008;180:4742-53.
$Gfap^{CreER}$	N/A	Casper KB, Jones K, McCarthy KD. Characterization of astrocyte-specific conditional knockouts. Genesis 2007;45:292-9.
$Rosa26^{TdTomato}$	007909	Madisen L, Zwingman TA, Sunkin SM, et al. A robust and high-throughput Cre reporting and characterization system for the whole mouse brain. Nature Neuroscience 2010;13:133-40.
$Rosa26^{LacZ}$	003474	Soriano P. Generalized lacZ expression with the ROSA26 Cre reporter strain. Nature Genetics 1999;21:70-1.
$Gfap^{Cre}$	012886	Garcia AD, Doan NB, Imura T, et al. GFAP-expressing progenitors are the principal source of constitutive neurogenesis in adult mouse forebrain. Nature Neuroscience 2004;7:1233-41.
$Gfap^{HSV-TK}$	005698	Bush TG, Savidge TC, Freeman TC, et al. Fulminant jejuno-ileitis following ablation of enteric glia in adult transgenic mice. Cell 1998;93:189-201.

N/A: Not applicable

Supplemental Table 2: Primary Antibodies

Antibody	Vendor	Catalogue Number	Dilution
Chicken anti-NFH	Millipore	AB5539	1:2500
Rabbit anti-S100β	DAKO	Z0311	1:500
Rabbit anti-Ki67	Abcam	ab15580	1:1000
Goat anti-HSV1 TK	Santa Cruz	sc-28038	1:200
Rabbit anti-GFAP	Sigma	G9269	1:1000
Chicken anti-GFAP	Millipore	AB5541	1:1000
Human anti-ANNA-1	Mayo Clinic	Gift from V. Lennon	1:40,000
Rabbit anti-PH2A.X	Cell Signaling	9718P	1:200
Rabbit anti-nNOS	ImmunoStar	24287	1:1500
Rabbit anti PGP9.5	Cedarlane	CL95101	1:1000
Rabbit anti-ZO-1	Invitrogen	61-7300	1:100
Rat anti-E-cadherin	Invitrogen	13-1900	1:100
Goat anti-SCFR	R&D Systems	AF1356	1:500

Supplemental Table 3: Previous studies of enteric glial disruption in mice

Epithelial function		
Approach	**Phenotype**	**Reference**
Chemical: Gliotoxin 6-aminonicotinamide	Ultrastructure of colonic epithelium was normal in mice treated with 6-aminonicotinamide.	1
Chemical: Gliotoxin fluorocitrate reversibly disrupts glial glucose uptake	No histological evidence of inflammation in wildtype mice treated with fluorocitrate for 7 days. Colonic epithelial permeability measured in Ussing chambers was not different between vehicle and fluorocitrate-treated mice.	2
Genetic: Acute ablation of expression of connexin-43, a gap junction protein, in Sox10-expressing cells	Colonic epithelial permeability was measured in Ussing chambers, and was not different between control and conditional knock-out mice.	3
Chemogenetic: Activation of DREADDs [designer receptors exclusively activated by designer drugs] within GFAP-expressing cells	Colonic epithelial permeability was measured in Ussing chambers, and was not different upon CNO (DREADD ligand) treatment between DREADD-expressing mice and control mice.	3
GI motility		
Approach	**Phenotype**	**Reference**
Chemical: Gliotoxin 6-aminonicotinamide	Mice treated with 6-aminonicotinamide developed diarrhea. Transit time was not measured. Ultrastructure of enteric neurons was normal.	1
Chemical: Gliotoxin fluorocitrate	Small intestinal motility was slowed in fluorocitrate-treated mice relative to controls. Colonic bead expulsion time was unchanged.	2
Genetic: Acute ablation of connexin-43 in GFAP-expressing cells	Total GI transit time and 1 hour fecal pellet production were not different between control and conditional knock-out mice. Colonic bead expulsion was slower in conditional knock-outs.	4
Chemogenetic: Activation of DREADDs within GFAP-expressing cells	Transgenic DREADD mice and wildtype control mice were treated with the ligand CNO, and GI motility was measured. Total GI transit time and upper GI transit were not different, but 1 hour fecal pellet production increased and colonic bead expulsion was faster. *Ex vivo*, CMMC frequency, speed and amplitude all increased slightly.	5

Relevant References:

1. Aikawa H, Suzuki K. Enteric gliopathy in niacin-deficiency induced by CNS glio-toxin. Brain Res 1985;334:354-6.
2. Nasser Y, Fernandez E, Keenan CM, et al. Role of enteric glia in intestinal physiology: effects of the gliotoxin fluorocitrate on motor and secretory function. Am J Physiol Gastrointest Liver Physiol 2006;291:G912-27.
3. Grubisic V, Gulbransen BD. Enteric glial activity regulates secretomotor function in the mouse colon but does not acutely affect gut permeability. J Physiol 2017.
4. McClain JL, Grubisic V, Fried D, et al. Ca2+ responses in enteric glia are mediated by connexin-43 hemichannels and modulate colonic transit in mice. Gastroenterology 2014;146:497-507 e1.
5. McClain JL, Fried DE, Gulbransen BD. Agonist-evoked Ca2+ signaling in enteric glia drives neural programs that regulate intestinal motility in mice. Cell Mol Gastroenterol Hepatol 2015;1:631-645.

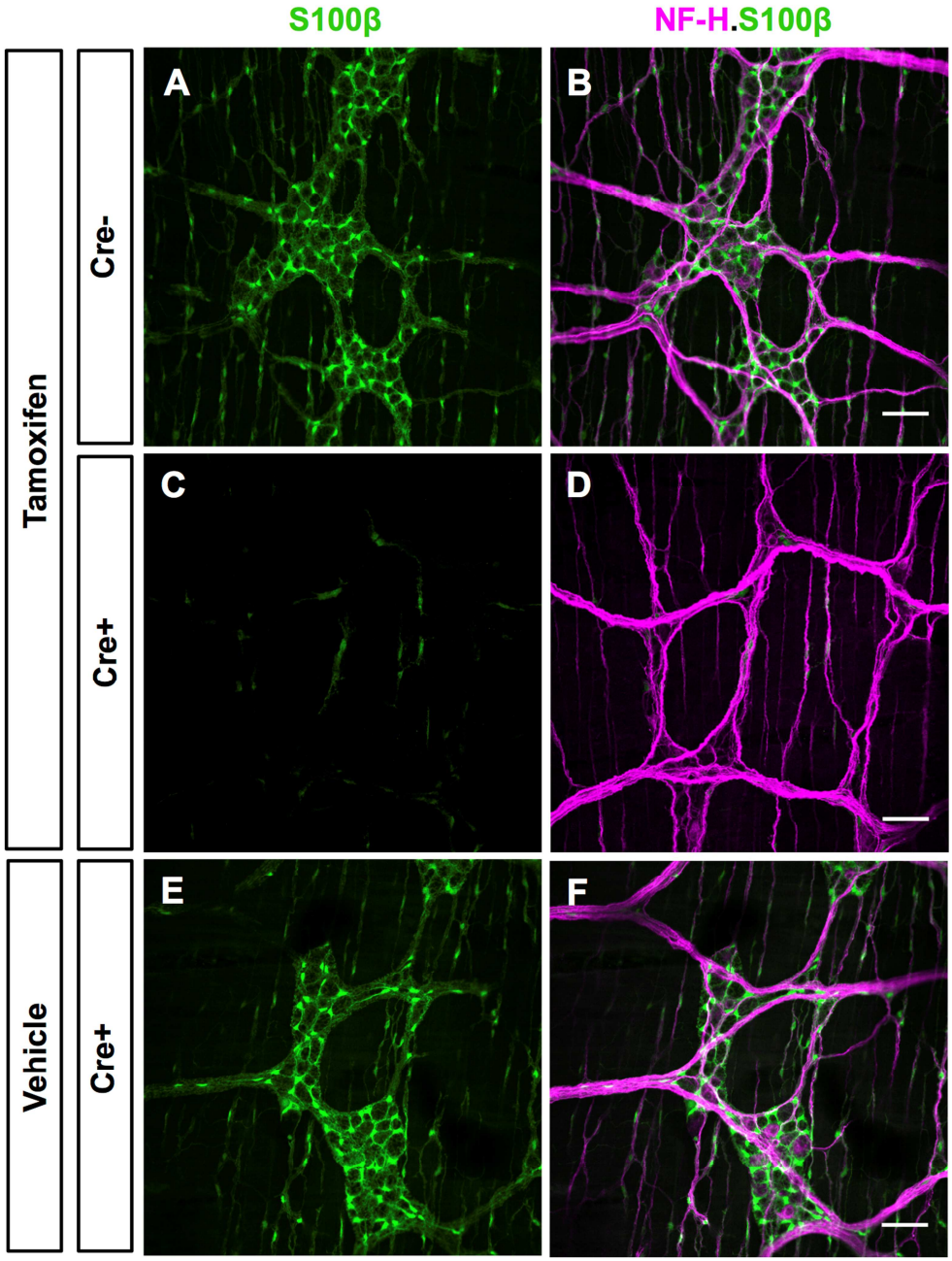
S100β
NF-H.S100β
Tamoxifen
Vehicle
Cre-
Cre+
Cre+
A
B
C
D
E
F

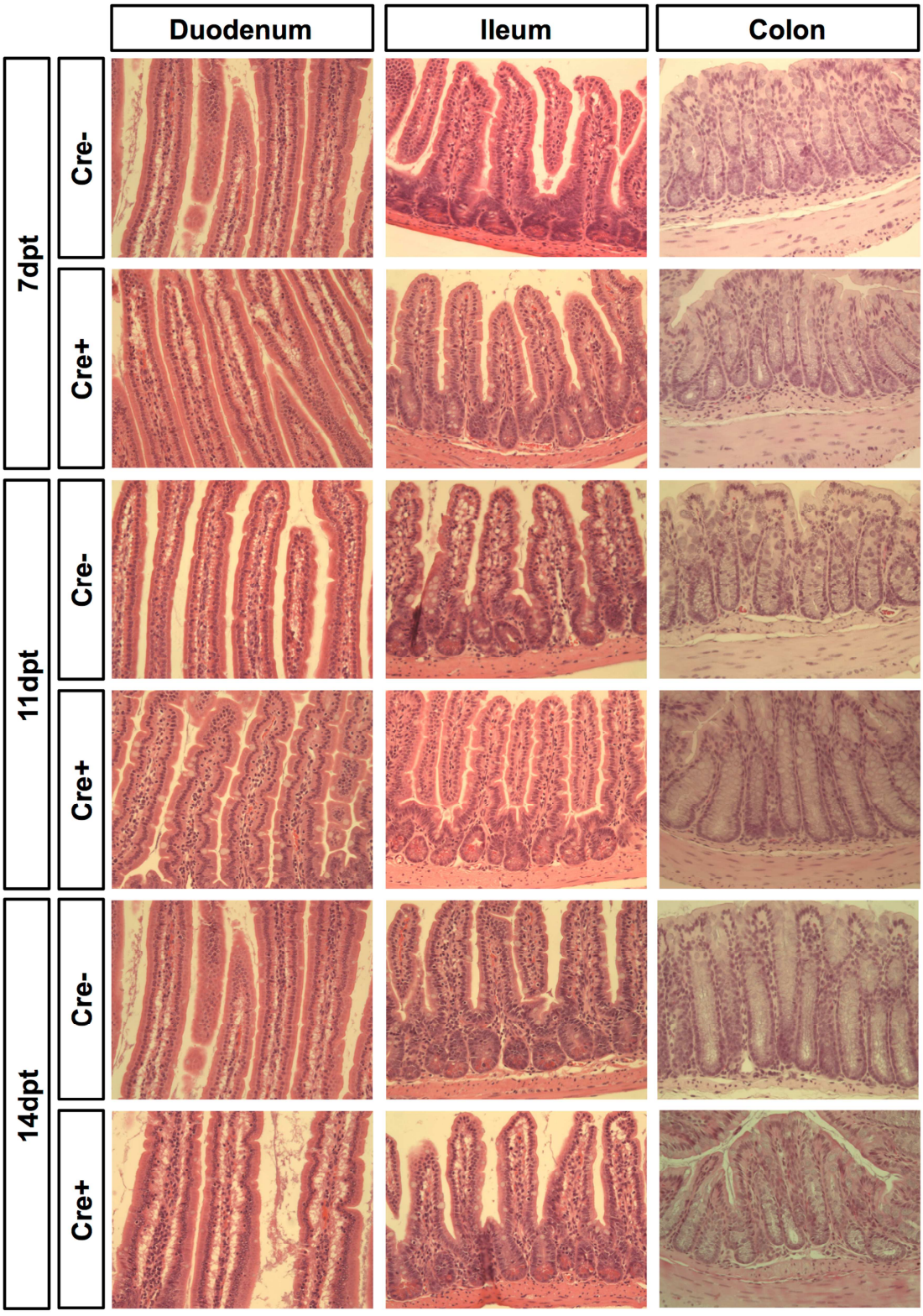
Duodenum
Ileum
Colon
7dpt
11dpt
14dpt
Cre-
Cre+
Cre-
Cre+
Cre-
Cre+

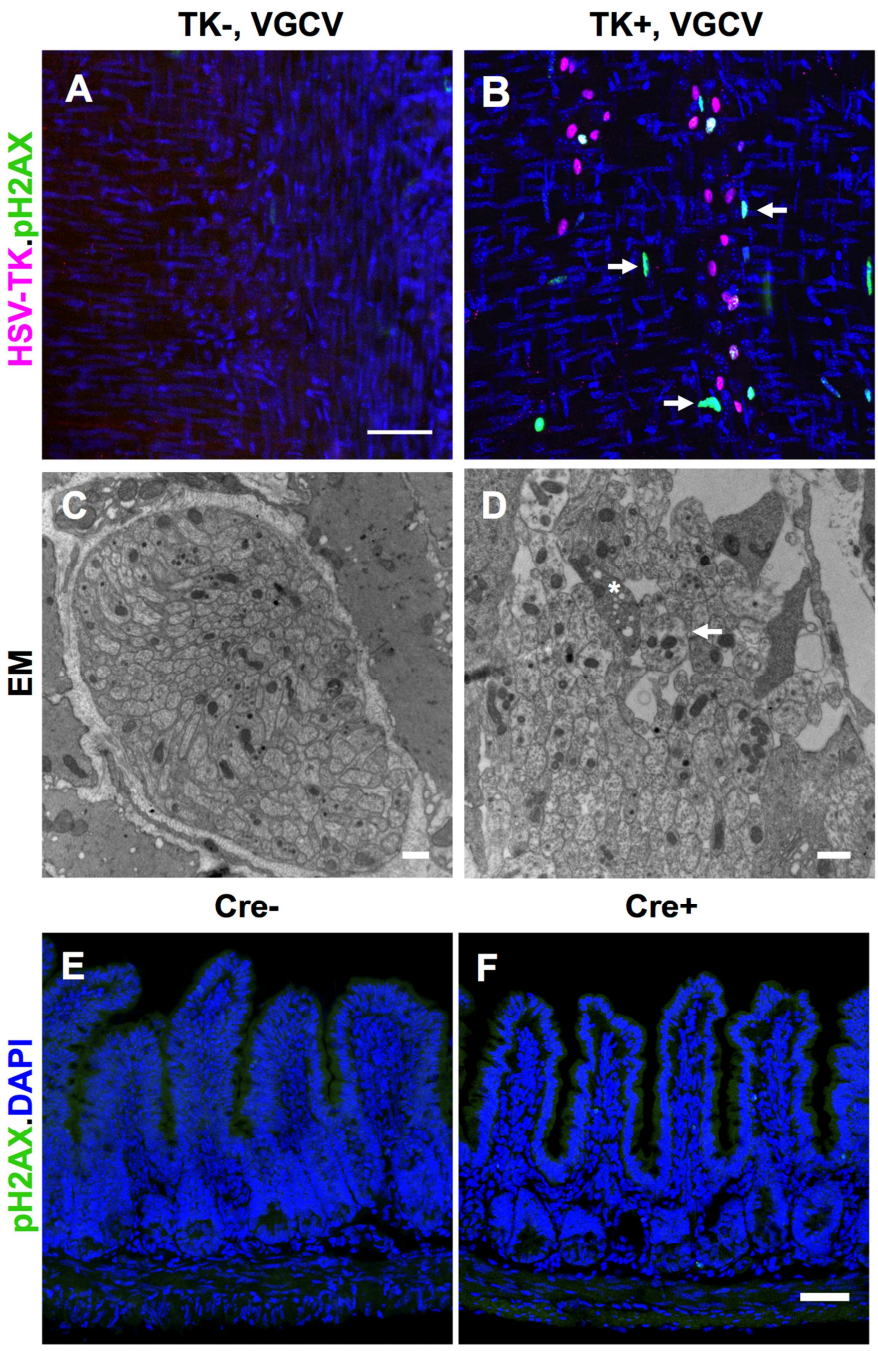
TK-, VGCV
TK+, VGCV
A
B
HSV-TK.pH2AX
C
D
EM
Cre-
Cre+
E
F
pH2AX.DAPI